Biosensors and Bioelectronics 58 (2014) 374–379

Contents lists available at ScienceDirect

Biosensors and Bioelectronics

journal homepage: www.elsevier.com/locate/bios

Surface plasmon resonance technique for directly probing the interaction of DNA and graphene oxide and ultra-sensitive biosensing

Tianyu Xue [a], Xiaoqiang Cui [a,*], Weiming Guan [b], Qiyu Wang [a], Chang Liu [a], Haitao Wang [a], Kun Qi [a], D.J. Singh [c], Weitao Zheng [a,**]

[a] Key Laboratory of Automobile Materials of MOE and State Key Laboratory of Superhard Materials, Department of Materials Science, Jilin University, Changchun 130012, People's Republic of China
[b] State Key Laboratory of Advanced Technologies for Comprehensive Utilization of Platinum Metals, Kunming 650106, People's Republic of China
[c] Materials Science and Technology Division, Oak Ridge National Laboratory, Oak Ridge, TN 37831-6056, United States

ARTICLE INFO

Article history:
Received 6 January 2014
Received in revised form
20 February 2014
Accepted 1 March 2014
Available online 12 March 2014

Keywords:
DNA
Graphene oxide
Hydrogen bond
Surface plasmon resonance
Au nanoparticles

ABSTRACT

The binding of DNA with graphene oxide (GO) is important for applications in disease diagnosis, genetic screening, and drug discovery. The standard assay methods are mainly limited to indirect observation via fluorescence labeling. Here we report the use of surface plasmon resonance for direct sensing of DNA/GO binding. We show that this can be used for ultra-sensitive detection of single-stranded DNA (ssDNA). Furthermore, the results provide a more direct probe of DNA/GO binding abilities and confirm that hydrogen bonding plays a key role in the interaction between GO and ssDNA. This enables to a novel biosensor for highly sensitive and selective detection of ssDNA based on indirect competitive inhibition assay (ICIA). We report development of such a sensor with a linear dynamic range of 10^{-14}–10^{-6} M, a detection limit of 10 fM and a high level of stability during repeated regeneration.

1. Introduction

The interactions of DNA with graphene oxide (GO) are of key importance in materials science, nanotechnology, biosensing, and biomedicine (Chen et al., 2013; Loh et al., 2010; Min et al., 2011; Ocsoy et al., 2013; Tang et al., 2013; Zhu et al., 2013b). There are many assays for molecular interactions with surfaces. However, the most successful surface-based affinity tools are based on fluorescence (Lee et al., 2007; Murphy et al., 2009; Smith et al., 1986; Zhu et al., 2013a). GO has been extensively used as the quencher in single-stranded DNA (ssDNA) sensing (Huang et al., 2012b; Lu et al., 2009; Wang et al., 2012a, 2012b, 2013a). This method requires a complex fluorescent substance labeling procedure and special molecular biological facilities. These significantly increases the cost and difficulty of the analyses (Yang et al., 2013). Development of sensitive, simple and low-cost methods for direct observation of the binding of DNA with GO remains a challenge. Surface plasmon resonance (SPR) methods are sensitive optical techniques for monitoring biomolecular binding events via detection refractive index changes on a metal sensor surface (Cooper, 2002; Cui et al., 2003; Knoll, 1998). Our recent work showed that the SPR signal is very sensitive to the assembly and the change of the oxide state of GO nanosheets (Xue et al., 2013). This suggests GO-modified SPR chip surfaces could potentially be developed as platforms for sensing the interaction of DNA with GO.

Here we report the use of this technique to systematically study the different interaction strengths of ssDNA and dsDNA with GO. The results show that the interaction of ssDNA with GO is through hydrogen bonding. This is significant because it implies a strong different in binding between ssDNA and dsDNA, since one may expect a competition between the hydrogen bonding with the GO and the hydrogen bonding between the strands comprising the dsDNA. This is in contrast with the behavior that might be anticipated if the ssDNA–GO interaction mechanisms were primarily of pi-stacking or hydrophobic nature as has been assumed based e.g. on analogy with dsDNA (Loh et al., 2010; Lu et al., 2009; Ocsoy et al., 2013; Tang et al., 2012; Wang et al., 2010, 2013b). Importantly, this also means interaction between the GO and a plasmonic chip, and therefore the SPR can be potentially affected by the interaction of ssDNA with the GO. We show that this is the case.

We report the design and demostration of an excellect label free DNA sensor based on the above, in particular the high binding affinity of ssDNA and GO, using a GO-modified SPR chip. As mentioned, SPR has become a powerful technique for studying biomolecular interactions in fields of biology, food, medicine, and environment (Daniel et al., 2013; Nelson et al., 2000; Šípová and Homola, 2013). Unfortunately, the inability of the conventional SPR instruments to measure

* Corresponding author. Tel./fax: +86 431 85155279.
** Corresponding author. Tel./fax: +86 431 85165246.
E-mail addresses: xqcui@jlu.edu.cn (X. Cui), wtzheng@jlu.edu.cn (W. Zheng).

http://dx.doi.org/10.1016/j.bios.2014.03.002
0956-5663/

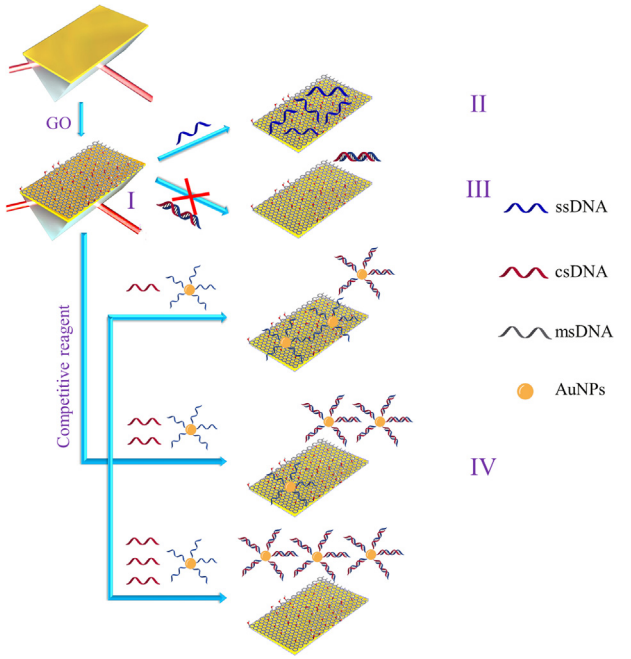

Scheme 1. Schematic illustration of the procedure for ssDNA detection based on the ssDNA/dsDNA discrimination ability of GO, with utilization of AuNPs–ssDNA conjugates as a competitive reagent.

extremely small changes in refractive index has hindered applications in ultrasensitive bioanalysis (Cui et al., 2005; Pei et al., 2001; Szunerits et al., 2013). The traditional detection of target ssDNA via its hybridization with a probe immobilized on the SPR sensor surface is usually referred to as direct detection (Goodrich et al., 2004). The typical limit of detection (LOD) of ssDNA in direct detection is in the nanomolar or subnanomolar range depending on the target size, hybridization conditions and the particular SPR platform (Carrascosa et al., 2009; Milkani et al., 2010; Šípová and Homola, 2013; Šípová et al., 2010; Wang et al., 2011). To improve the sensitivity of DNA sensor, we developed an ultra-sensitive DNA detecion platform using the SPR technique by combining GO and gold nanoparticles (AuNPs) based on indirect competitive inhibition assay (ICIA).

The principle of the present strategy is schematically illustrated in Scheme 1. GO is self-assembled on the SPR chip surface through the strong metal-carbon coupling between GO and gold film. The fact that ssDNA exhibits dramatic higher binding ability to GO surface than dsDNA is the key point that is exploited by the designs (II and III). We exploit the coupling of the localized-SPR (LSPR) of the nanoparticles and the propagating-SPR of the gold film (Chang et al., 2012; Yuan and Li, 2009; Yuan et al., 2011, 2013; Zheng et al., 2011). The AuNPs–ssDNA is employed as a competitive reagent to amplify the SPR signal (IV) (Hu et al., 2013). The biosensor could then detect target complementary single strand DNA (csDNA) in a linear dynamic range of 10^{-14}–10^{-6} M using the HIV-1 U5 long terminal repeat sequence DNA as a model system (Lu et al., 2009; Zhang et al., 2012). AuNPs–ssDNA conjugates as a powerful competitive receptors and provide an LOD of 10 fM, which is 7 order of the magnitude lower than that without AuNPs.

2. Experimental section

2.1. Materials

The ssDNA probe of HIV-1 U5 long terminal repeat sequence (5′SH-AGT CAG TGT GGA AAA TCT CTA GC 3′), complementary strand sequence (5′GCT AGA GAT TTT CCA CAC TGA CT 3′) and the mismatch sequence (5′GCT AGA GAT TGT CCA CAC TGA CT 3′) was synthesized by Shanghai Sangon Biotechnology Co., Ltd. (Shanghai, China). Graphene oxide was prepared by previously described method.

2.2. Preparation of 14 nm AuNPs

Trisodium citrate (25 mL, 38.8 mM) was added to a boiling solution of HAuCl4 (250 mL, 1 mM). Within several minutes, the color of the solution changed from pale yellow to deep red. The mixture was refluxed for 30 min to ensure complete reduction and then slowly cooled to room temperature. The preparation of AuNPs is characterized by TEM image (Fig. S1a).

2.3. Preparation of DNA-complexed gold nanoparticles

In a typical preparation, the gold nanoparticles were conjugated with thiolated single-stranded oligonucleotides by incubating a gold solution (3 mL, 6 nM) overnight with disulfide-protected oligonucleotides (150 μL, 40 μM) in aqueous solution. Then the solution was diluted to a final volume of 6 mL containing NaCl (0.2 M) and PBS (0.01 M, pH 7.0). After further incubation for 2 h the volume was slowly reduced to 900 μL by vacuum centrifugation over 5–6 h at 40 °C. Unbound oligonucleotides were then removed by repeated centrifugation and suspension of the pellet. The AuNPs–ssDNA were stored in a solution (3 mL) containing NaCl (0.2 M) and PBS (0.01 M, pH 7.0). The preparation of AuNPs–ssDNA was characterized by UV–vis spectra (Fig. S1b).

2.4. Instrumentation

Transmission electron-microscope (TEM) images were taken with a Hitachi H-8100 IV instrument operating at 200 kV (FEI Co., USA). AFM images were obtained with ScanAsyst in Air mode on a Bruker Dimension Icon scanning probe microscope (Bruker Co., Germany). The thickness and surface coverage of the GO sheets assembled on Au films were got with Bearing analysis on an AFM software (NanoScopeAnalysis). The formation of the DNA-nanoparticle conjugates was supported by UV–vis spectroscopy (200–800 nm, CHEMUSB4000-UV/vis, Ocean Optics Inc.). SPR spectrometry was carried out using a TR2005 spectrometer (RES-TEC resonant sensor technology, Germany). The set-up was based on the conventional Kretchmann configuration and included a He–Ne laser of wavelength $\lambda = 632.8$ nm which was coupled to the system via a high refractive index prism, LAFSN9 glass $\varepsilon = 3.40$. The gold-coated sensor chip mounted with a homemade electrochemical flow cell was attached to the prism with high index matching oil. The reflected light was detected by a photodiode. Cyclic voltammetry experiments were carried out in PBS (pH 7.4) on a CHI650D electrochemical workstation (Shanghai, Chenhua Co., China). A three-electrode cell was used with gold film as the working electrode, a AgCl electrode as the reference electrode, and a platinum electrode as the counter-electrode. All experiments were done at room temperature.

2.5. Detection format

For the detection of target ssDNA, an indirect competitive inhibition method was used. In this assay, the AuNPs–ssDNA was incubated with different concentrations of target csDNA for 30 min. The hybridization buffer was a solution of PBS (0.01 M) containing NaCl (0.2 M). After that, the mixing solution was injected to SPR cell for 15 min to let the free ssDNA bind the GO surface. Afterwards, the sensor surface was washed with PBS.

3. Results and discussion

Single layer GO was assembled and electrochemically reduced in situ on SPR chips, as described in the previous reports.(Chen et al., 2012; Hummers and Offeman, 1958; Wu et al., 2013b; Xue et al., 2013) The morphological changes of the sensor chip surface were characterized by AFM, as shown in Fig. 1a–c. The thickness and surface coverage of the GO sheets assembled on Au films were 2.2 nm and 72.6 ± 7.9%, respectively, which confirms the successful assembly of the GO on the Au sensor chip (Huang et al., 2012a). The surface coverage decreases slightly to 69.1 ± 7.9% with an in-situ electrochemical reduction (Fig. 1c). Thus the loss of GO was not significant after application of the high electrochemical reduction potential. The reduction of GO was characterized by XPS and contact angle technique (as shown in Figs. S2 and S3). Single layer GO nanosheets were also characterized by TEM, which shows that the as-prepared GO consists of well-dispersed wrinkled and folded flakes with the same size as AFM results (as shown in Fig. S4).

The SPR angle reflectivity spectrum is very sensitive to small changes of the refractive index on the sensor chip surface.(Knoll, 1998; Riskin et al., 2009) An injection of the ssDNA solution over the GO surface results in an immediate increase of the SPR signal, which reaches a plateau after 5 min (inset of Fig. 2a). This indicates that fast binding occurs between ssDNA and GO surface. The different binding abilities of ssDNA and dsDNA to GO or electrochemically reduced GO (ERGO) surfaces were investigated by monitoring the changes of SPR angles ($\Delta\theta$) while injecting a series of concentrations of ssDNA and dsDNA on both substrates (as shown in Fig. 2a and c). It is clear from Fig. 2a that the binding tendency of ssDNA to GO is much higher than dsDNA. For instance,

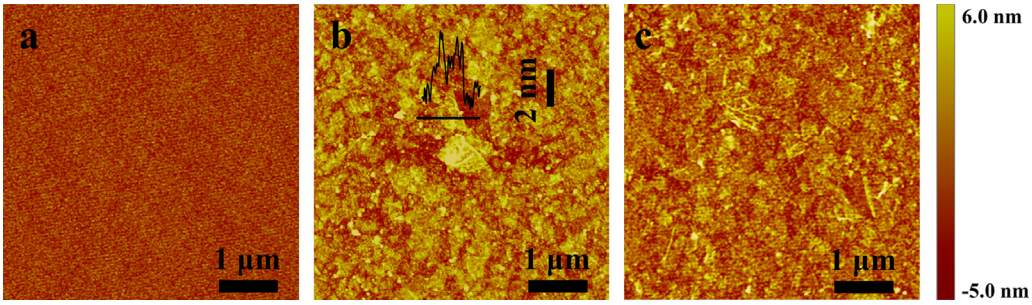

Fig. 1. AFM images of bare Au film (a), GO assembled on a Au film (b) and ERGO on a Au film (c).

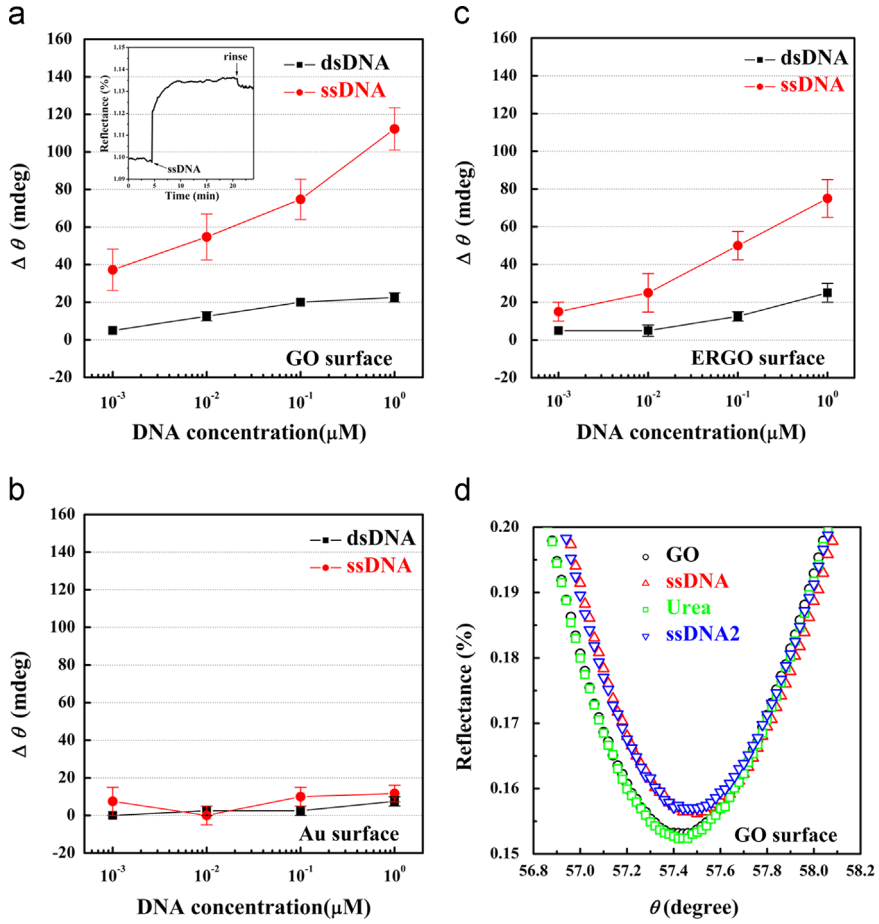

Fig. 2. Relationship between resonance angle shift and ssDNA/dsDNA concentration on GO (a), Au (b), and ERGO (c) substrates. Each point corresponds to the average value of the SPR angle shift for the concentration of ssDNA/dsDNA. Regenerations experiment for ssDNA using 4 M urea (d). The inset of (a) shows the real-time SPR response for ssDNA adsorption onto the GO surface. (For interpretation of the references to color in this figure, the reader is referred to the web version of this article.)

the adsorption of 10^{-3} μM ssDNA onto the GO surface results in an SPR angle shift of 37.25 ± 10 mdeg, which is seven times higher than that of the dsDNA. These results directly show that the hybridization significantly inhibits the binding of DNA to the GO surface (Lu et al., 2009; Xue et al., 2013). In control experiments, both ssDNA and dsDNA show undetectable $\Delta\theta$ on Au substrates (Fig. 2b).

The surface of GO contains several functional groups and domains (polar hydroxy and epoxide groups, carboxylate groups and π-bonds). There are three mechanisms that can be involved in the interaction of DNA and graphene, namely hydrogen bonding, pi-stacking, and hydrophobic.(Loh et al., 2010; Lu et al., 2009; Ocsoy et al., 2013; Tang et al., 2012; Wang et al., 2010, 2013b). The SPR signal from dsDNA does not show significant differences between GO and ERGO surfaces, with a response of about 20 m deg for 1 μM dsDNA (black curves in Fig. 2a and c), indicating that pi-stacking, and hydrophobic interactions mainly contribute to the binding of dsDNA to graphene. ERGO has higher pi interactions and is more hydrophobic than GO. Thus, if the main driving force is attributed to the pi-stacking or hydrophobic interactions, (Loh et al., 2010; Lu et al., 2009; Ocsoy et al., 2013; Tang et al., 2012; Wang et al., 2010,2013b) the binding affinities of ssDNA–ERGO should be stronger than those for ssDNA–GO. However,the SPR response from ssDNA–ERGO is only ca. the half of that from ssDNA–GO (red curves in Fig. 2a and c). This indicates that the primary driving force for the ssDNA–GO interaction is hydrogen bonding rather than pi-stacking or hydrophobic interactions. To test this we used urea to disrupt the hydrogen bonding (Fig. 2d) (Park et al., 2013). The SPR response decreases to the original state of GO after an incubation with 4 M urea for 10 min. This indicates a suppression of the binding of ssDNA with the GO surface by urea. The SPR response of characteristic of the normal binding could be restored by incubating with ssDNA, as shown in the blue curve (ssDNA2 in Fig. 2). This binding-regeneration process could be repeated tens of times by alternately incubating the GO surface with ssDNA and urea solution. This result not only confirms that the interaction between GO and ssDNA is mainly due to hydrogen bonding, but also provides a method for regeneration for GO-modified SPR chip for repeatable sensing.

As mentioned, dsDNA binds only weakly onto the GO surface, in contrast to ssDNA, which is hydrogen bonded to the GO. Adsorption of ssDNA onto GO is blocked by the addition of csDNA, leading to the formation of dsDNA from a matched ssDNA. Thus an indirect competitive inhibiting strategy for a SPR biosensor can be used to detect a particular sequence of ssDNA on a non-specific binding substrate of GO (Scheme 1) (Wang et al., 2009). The SPR signal can be further amplified using AuNPs, which exhibit LSPR and provide a high refractive index change (Knez et al., 2012; Lyon et al., 1998; Tan et al., 2013; Wu et al., 2013a). An AuNPs–ssDNA conjugate was used to amplify the original SPR signal of ssDNA binding.(He et al., 2010; Li et al., 2013) As shown in Fig. 3, the binding of AuNPs–ssDNA onto GO through hydrogen bonding (Park et al., 2013) results in a significant increase of 130 mdeg in the SPR angle (yellow squares) (He et al., 2010). The SPR angle showed a left-shift of 90 mdeg (red inverted triangles) after an AuNPs–ssDNA conjugates solution was mixed with 1 μM of csDNA. This indicates that the target csDNA hybridized with AuNPs–ssDNA and inhibited its hydrogen bonding interaction with GO. When the mismatched ssDNA (msDNA, 1 μM) was used, the SPR angle shifted slightly right (gray triangles) relative to that of AuNPs–ssDNA (Bonanni and Pumera, 2011). This observation indicates that the msDNA also bound to the GO-based SPR chip surface instead of inhibiting the binding of AuNPs–ssDNA conjugates. Thus opposite signals are obtained for csDNA and msDNA.

The coupling between the LSPR of the AuNPs and the propagating SPR (PSPR) of the Au surface can be used to amplify SPR responses (Frasconi et al., 2010; Tang et al., 2013). Two series of

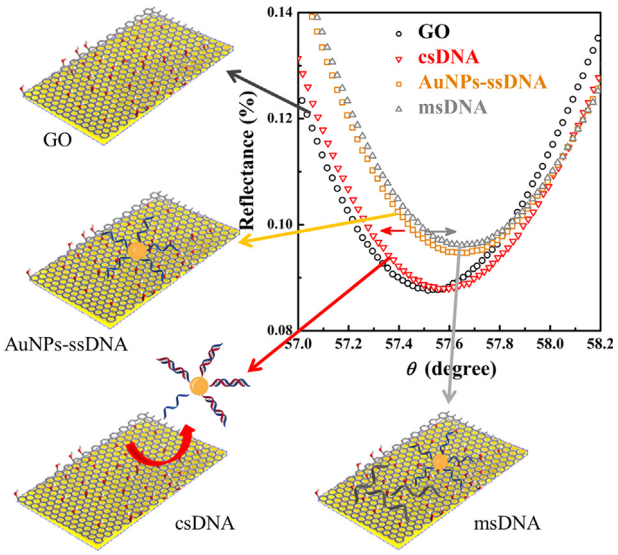

Fig. 3. Schematic of the protocol and SPR angular reflectivity spectra, reflectance versus θ for the GO (black), AuNPs–ssDNA (yellow), target complementary ssDNA (red), and mismatched ssDNA (gray). All measurements were performed in 0.01 M PBS buffer solution containing 0.2 M NaCl. (For interpretation of the references to color in this figure, the reader is referred to the web version of this article.)

experiments were performed using the same process with either AuNPs–ssDNA or ssDNA as the competitive reagent to illustrate this amplification. The SPR responses are shown in Fig. 4. In the case of the AuNPs–ssDNA, the hybridization of the target csDNA results in an obvious left-shift of the SPR angles even at a very low concentrations of 10^{-14} M. With the same process, but using non-modified-ssDNA as the competitive reagent, the left shifts of SPR angles are barely detectable for the same series of concentrations, indicating that SPR signal was enhanced by the electronic coupling between the LSPR of AuNPs and the PSPR associated with Au film.

The calibration curve for the SPR response versus csDNA concentration is shown in Fig. 5. The SPR signals from the non-modified-ssDNA competitive reagent are included for comparison. Fig. 5a shows that the sensor response (left-shift of SPR angles, $\Delta\theta$) is proportional to the concentration of the target csDNA with a linear relationship over the range of 10^{-14} M to 10^{-6} M with an LOD of 10 fM estimated according to the IUPAC guideline of 3:1 signal to noise of 1 mdeg. This is 10^7 times lower than that with a non-modified competitive reagent. One may note that in the bar graph the value for mismatched target ssDNA is negative. This is due to the fact that the SPR angle for msDNA shifts to the right intead of the left. Finally, the binding of AuNPs–ssDNA conjugates on the GO film can be regenerated by treating with urea (4 M for 15 min.), and with this regeneration protocol the interface could be used repeatedly to detect ssDNA (Fig. S5).

4. Conclusions

We used a surface plasmon resonance technique to directly investigate DNA/GO binding. The results show that hydrogen bonding plays a key role to the interaction between GO and ssDNA. However, the binding of dsDNA is different and weaker presumably due to competition between the interstrand binding in dsDNA and the binding with the GO. Based on this observation, we developed graphene-derived chip and demonstrate this as an improved DNA sensing platform. The biosensor, based on the principle of indirect competitive inhibition, exhibits a linear dynamic range of 10^{-14} M to 10^{-6} M for the detection of target csDNA (HIV-1 U5 long terminal repeat sequence). Ultra-sensitive

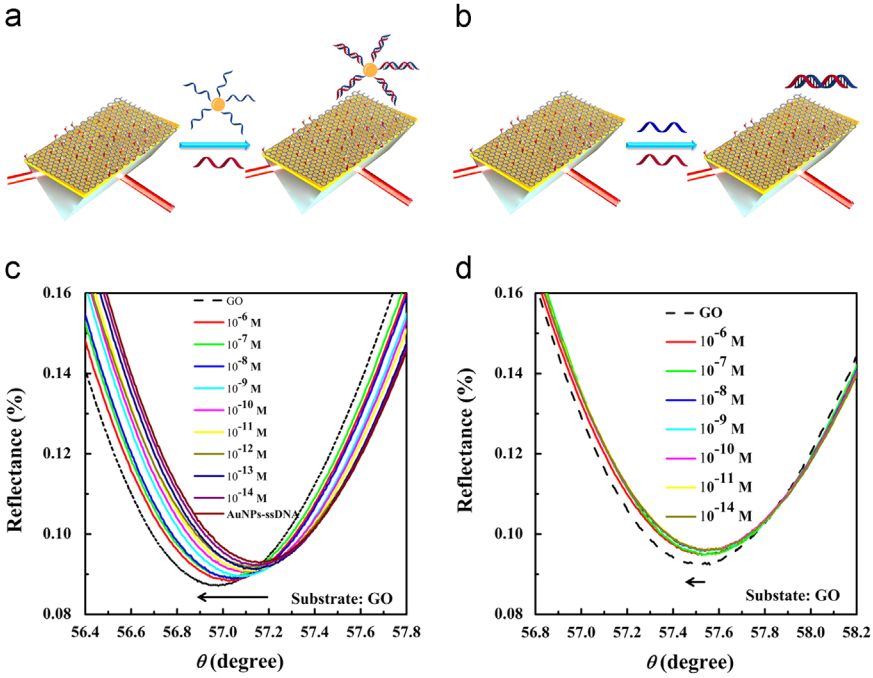

Fig. 4. Schematic illustration of different concentrations of target csDNA mixing with AuNPs–ssDNA (a) and ssDNA (b) as competitive acceptors. SPR angular reflectivity spectra for a GO-based SPR chip surface incubated with the mixing solution of AuNPs–ssDNA (c) and ssDNA (d) with 10^{-14}–10^{-6} M target csDNA.

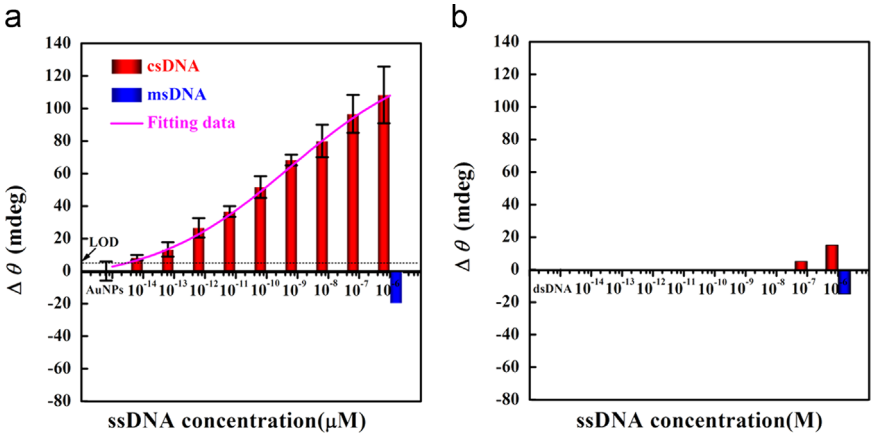

Fig. 5. The left-shift of SPR angles versus a series of concentrations of target csDNA (red) and msDNA mixing with AuNPs–ssDNA (a) and ssDNA (b) as competitive acceptor. (For interpretation of the references to color in this figure, the reader is referred to the web version of this article.)

ssDNA detection is achieved using the amplification effects of LSPR coupling from AuNPs and gold film. Using of AuNPs–ssDNA conjugates powerful competitive receptors provide a LOD as low as 10 fM in 10 mM PBS. Finally, this GO-based sensor surface displays a high level of stability over the course of repeated sensing and regeneration cycles.

Acknowledgments

This work was financially supported by the National Natural Science Foundation of China (Nos. 21275064, 21075051, and 51372095), Program for New Century Excellent Talents in University (NCET-10-0433), the State Key Laboratory of Advanced Technologies for Comprehensive Utilization of Platinum Metals (SKL-SPM-201207), the Fundamental Research Funds for the Jilin University (Grant no. 200903020), and the "211" and "985" Projects of Jilin University, China. Work at ORNL was supported by the Department of Energy, Basic Energy Sciences, Materials Sciences and Technology Division.

Appendix A. Supporting information

Supplementary data associated with this article can be found in the online version at http://dx.doi.org/10.1016/j.bios.2014.03.002.

References

Bonanni, A., Pumera, M., 2011. ACS Nano 5, 2356–2361.
Carrascosa, L.G., Calle, A., Lechuga, L.M., 2009. Anal. Bioanal. Chem. 393, 1173–1182.
Chang, S., Li, Q., Xiao, X., Wong, K.Y., Chen, T., 2012. Energy Environ. Sci. 5, 9444–9448.
Chen, J., Cui, X., Wang, Q., Wang, H., Zheng, X., Liu, C., Xue, T., Wang, S., Zheng, W., 2012. J. Colloid Interface Sci. 383, 140–147.
Chen, T.-Y., Loan, P.T.K., Hsu, C.-L., Lee, Y.-H., Tse-Wei Wang, J., Wei, K.-H., Lin, C.-T., Li, L.-J., 2013. Biosens. Bioelectron. 41, 103–109.
Cooper, M.A., 2002. Nat. Rev. Drug Discov. 1, 515–528.

Cui, X., Pei, R., Wang, Z., Yang, F., Ma, Y., Dong, S., Yang, X., 2003. Biosens. Bioelectron. 18, 59–67.
Cui, X., Yang, F., Li, A., Yang, X., 2005. Anal. Biochem. 342, 173–175.
Daniel, C., Roupioz, Y., Gasparutto, D., Livache, T., Buhot, A., 2013. PloS One 8, e75419.
Frasconi, M., Tel-Vered, R., Riskin, M., Willner, I., 2010. Anal. Chem. 82, 2512–2519.
Goodrich, T.T., Lee, H.J., Corn, R.M., 2004. J. Am. Chem. Soc. 126, 4086–4087.
He, S., Song, B., Li, D., Zhu, C., Qi, W., Wen, Y., Wang, L., Song, S., Fang, H., Fan, C., 2010. Adv. Funct. Mater. 20, 453–459.
Hu, W., Li, X., He, G., Zhang, Z., Zheng, X., Li, P., Li, C.M., 2013. Biosens. Bioelectron. 50, 338–344.
Huang, X., Qi, X., Boey, F., Zhang, H., 2012a. Chem. Soc. Rev. 41, 666–686.
Huang, X., Zeng, Z., Fan, Z., Liu, J., Zhang, H., 2012b. Adv. Mater. 24, 5979–6004.
Hummers, W.S., Offeman, R.E., 1958. J. Am. Chem. Soc. 801339
Knez, K., Janssen, K.P.F., Pollet, J., Spasic, D., Lammertyn, J., 2012. Small 8, 868–872.
Knoll, W., 1998. Annu. Rev. Phys. Chem. 49, 569–638.
Lee, C.-Y., Harbers, G.M., Grainger, D.W., Gamble, L.J., Castner, D.G., 2007. J. Am. Chem. Soc. 129, 9429–9438.
Li, L.-L., Wu, P., Hwang, K., Lu, Y., 2013. J. Am. Chem. Soc. 135, 2411–2414.
Loh, K.P., Bao, Q., Eda, G., Chhowalla, M., 2010. Nat. Chem. 2, 1015–1024.
Lu, C.-H., Yang, H.-H., Zhu, C.-L., Chen, X., Chen, G.-N., 2009. Angew. Chem. 121, 4879–4881.
Lyon, L.A., Musick, M.D., Natan, M.J., 1998. Anal. Chem. 70, 5177–5183.
Milkani, E., Morais, S., Lambert, C.R., McGimpsey, W.G., 2010. Biosens. Bioelectron. 25, 1217–1220.
Min, S.K., Kim, W.Y., Cho, Y., Kim, K.S., 2011. Nat. Nanotechnol. 6, 162–165.
Murphy, J.N., Cheng, A.K.H., Yu, H.-Z., Bizzotto, D., 2009. J. Am. Chem. Soc. 131, 4042–4050.
Nelson, B.P., Grimsrud, T.E., Liles, M.R., Goodman, R.M., Corn, R.M., 2000. Anal. Chem. 73, 1–7.
Ocsoy, I., Gulbakan, B., Chen, T., Zhu, G., Chen, Z., Sari, M.M., Peng, L., Xiong, X., Fang, X., Tan, W., 2013. Adv. Mater. 25, 2319–2325.
Park, J.S., Na, H.-K., Min, D.-H., Kim, D.-E., 2013. Analyst 138, 1745–1749.
Pei, R., Cui, X., Yang, X., Wang, E., 2001. Biomacromolecules 2, 463–468.
Riskin, M., Tel-Vered, R., Lioubashevski, O., Willner, I., 2009. J. Am. Chem. Soc. 131, 7368–7378.
Šípová, H., Homola, J., 2013. Anal. Chim. Acta 773, 9–23.
Šípová, H., Zhang, S., Dudley, A.E.M., Galas, D., Wang, K., Homola, J.I., 2010. Anal. Chem. 82, 10110–10115.
Smith, L.M., Sanders, J.Z., Kaiser, R.J., Hughes, P., Dodd, C., Connell, C.R., Heiner, C., Kent, S.B., Hood, L.E., 1986. Nature 321, 674–679.
Szunerits, S., Maalouli, N., Wijaya, E., Vilcot, J.-P., Boukherroub, R., 2013. Anal. Bioanal. Chem. 405, 1435–1443.
Tan, L.H., Xing, H., Chen, H., Lu, Y., 2013. J. Am. Chem. Soc. 135, 17675–17678.
Tang, L., Chang, H., Liu, Y., Li, J., 2012. Adv. Funct. Mater. 22, 3083–3088.
Tang, L., Chun, I.S., Wang, Z., Li, J., Li, X., Lu, Y., 2013. Anal. Chem. 85, 9522–9527.
Wang, J., Munir, A., Zhou, H.S., 2009. Talanta 79, 72–76.
Wang, L., Zhu, C., Han, L., Jin, L., Zhou, M., Dong, S., 2011. Chem. Commun. 47, 7794–7796.
Wang, L., Zhu, J., Han, L., Jin, L., Zhu, C., Wang, E., Dong, S., 2012a. ACS Nano 6, 6659–6666.
Wang, Q., Cui, X., Chen, J., Zheng, X., Liu, C., Xue, T., Wang, H., Jin, Z., Qiao, L., Zheng, W., 2012b. RSC Adv. 2, 6245–6249.
Wang, S., Qiao, L., Zhao, C., Zhang, X., Chen, J., Tian, H., Zheng, W., Han, Z., 2013a. New J. Chem. 37, 1616–1622.
Wang, Y., Li, Z., Hu, D., Lin, C.-T., Li, J., Lin, Y., 2010. J. Am. Chem. Soc. 132, 9274–9276.
Wang, Y., Li, Z., Weber, T.J., Hu, D., Lin, C.-T., Li, J., Lin, Y., 2013b. Anal. Chem. 85, 6775–6782.
Wu, P., Hwang, K., Lan, T., Lu, Y., 2013a. J. Am. Chem. Soc. 135, 5254–5257.
Wu, S., He, Q., Tan, C., Wang, Y., Zhang, H., 2013b. Small 9, 1160–1172.
Xue, T., Cui, X., Chen, J., Liu, C., Wang, Q., Wang, H., Zheng, W., 2013. ACS Appl. Mater. Interfaces 5, 2096–2103.
Yang, Y., Yuan, L., Fang, X., Liang, X., Yang, F., 2013. Biosens. Bioelectron. 46, 80–83.
Yuan, W., Li, C.M., 2009. Langmuir 25, 7578–7585.
Yuan, W., Lu, Z., Li, C.M., 2011. J. Mater. Chem. 21, 5148–5155.
Yuan, W., Lu, Z., Wang, H., Li, C.M., 2013. Phys. Chem. Chem. Phys. 15, 15499–15507.
Zhang, L., Guo, S., Dong, S., Wang, E., 2012. Anal. Chem. 84, 3568–3573.
Zheng, X.T., Hu, W., Wang, H., Yang, H., Zhou, W., Li, C.M., 2011. Biosens. Bioelectron. 26, 4484–4490.
Zhu, C., Zeng, Z., Li, H., Li, F., Fan, C., Zhang, H., 2013a. J. Am. Chem. Soc. 135, 5998–6001.
Zhu, X., Sun, L., Chen, Y., Ye, Z., Shen, Z., Li, G., 2013b. Biosens. Bioelectron. 47, 32–37.